


# Examination of different features of fission fragments of the excited compound nucleus $^{236}\text{Np}$ produced in the $p + ^{235}\text{U}$ reaction at $10.3 \leq E_p \leq 30.0$ MeV within a stochastic approach

H. Eslamizadeh \**Department of Physics, Faculty of Nano and Bio Science and Technology, Persian Gulf University, 75169 Bushehr, Iran*

(Received 20 May 2021; accepted 9 August 2021; published 1 September 2021)

A stochastic approach based on four-dimensional Langevin equations has been used to estimate the mass distributions of fission fragments, the average masses of heavy fragments, the average total kinetic energies of fragments, and the average number of neutrons emitted per fission of  $^{236}\text{Np}$  produced in the  $p + ^{235}\text{U}$  reaction at  $10.3 \leq E_p \leq 30.0$  MeV. Three collective shape coordinates plus the projection of total spin of the compound nucleus to the symmetry axis  $K$  were considered in the four-dimensional dynamical model. The effects of shell corrections and dissipation coefficient of  $K$   $\gamma_K$  were considered in the dynamical calculations. Comparison of the theoretical results for the mass distributions of fission fragments, the average masses of heavy fragments, and the average number of neutrons emitted per fission with the experimental data showed that the results of calculations were in good agreement with the experimental data, although the results of calculations for the average total kinetic energies of fission fragments were slightly higher than the experimental data. It was also shown that the number of fission events increased with time, and almost all of the fission events occurred dynamically until  $t = 4 \times 10^{-18}$  s and that the number of fission events became saturated. Furthermore, it was also shown that the average masses of heavy fragments and the average total kinetic energies of fission fragments of  $^{236}\text{Np}$  decreased with increasing projectile energy.

DOI: [10.1103/PhysRevC.104.034601](https://doi.org/10.1103/PhysRevC.104.034601)

## I. INTRODUCTION

The discovery of nuclear fission [1,2] opened an important chapter in the nuclear physics. Although the phenomenon of nuclear fission has been discovered since about 80 yr back, the study of fission is still of general interest. Fission may take place in any of the heavy nuclei after capture of light particles or  $\gamma$  quanta. Statistical and dynamical descriptions of the fission process were often used to explain different fission characteristics (see, for example, Refs. [3–20]). During the past three decades the dynamical models based on the set of multidimensional Langevin equations have been used to determine different features of nuclear fission of the excited compound nuclei. One-, two-, three-, four- (4D), and five-dimensional Langevin calculations usually have been used to simulate the fission of the excited compound nuclei (see, for example, Refs. [21–34]). The main motivation of this paper is to study the ability of the 4D dynamical model to simulate fission dynamics of the excited compound nucleus  $^{236}\text{Np}$  produced in the  $p + ^{235}\text{U}$  reaction at  $10.3 \leq E_p \leq 30.0$  MeV. It should be mentioned that many authors in simulation of the fission process of the excited compound nuclei assumed that the magnitude of projection of total spin of the compound nucleus about the symmetry axis is zero where this assumption is not correct [35,36]. Therefore, in the present research the dynamical evolution of the projection of total spin of the compound nucleus about the symmetry axis is considered

to calculate the mass distributions of fission fragments, the average masses of heavy fragments, the average total kinetic energies of fragments, and the average number of neutrons emitted per fission of  $^{236}\text{Np}$  produced in the  $p + ^{235}\text{U}$  reaction at  $10.3 \leq E_p \leq 30.0$  MeV.

The present paper has been arranged as follows: The model and basic equations are described in Sec. II. The results of calculations are presented in Sec. III. Finally, the concluding remarks are given in Sec. IV.

## II. DETAILS OF THE MODEL AND BASIC EQUATIONS

In the 4D dynamical model, evolution of a compound nucleus from the spherical shape to the scission point can be considered by the two-center shell-model shape parametrization [37]. The collective shape coordinates in the two-center parametrization are  $(q_1, q_2, q_3) = (r/R_0, \eta, \alpha)$  where  $r$  is the distance between two potential centers,  $R_0$  is the radius of spherical compound nucleus, parameter  $\alpha = (A_1 - A_2)/(A_1 + A_2)$  describes the mass asymmetry of the two fragments, where  $A_1$  and  $A_2$  are the mass numbers of fragments. The parameter  $\eta$  denotes the deformation of the fragments and is defined as  $\eta_i = 3(a_i - b_i)/(2a_i + b_i)$  with  $i = 1, 2$  for each fragment. Parameters  $a_i$  and  $b_i$  are the half length of the axes of an ellipse in the  $z$  and  $\rho$  directions of the cylindrical coordinate as shown in Fig. 1. It should be mentioned that in the present research, is assumed that the shape of the fission fragment tips of the left and right fragments to be the same ( $\eta = \eta_1 = \eta_2$ ).

\*Corresponding author: [eslamizadeh@pgu.ac.ir](mailto:eslamizadeh@pgu.ac.ir)

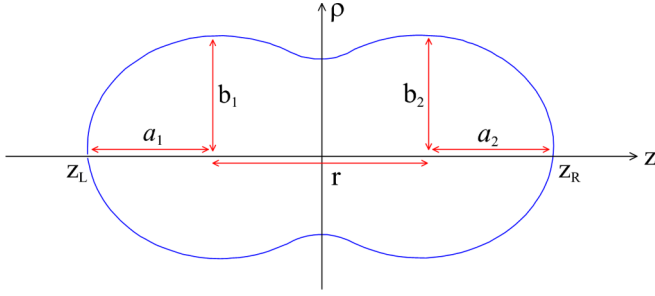


FIG. 1. Shape parametrizations based on the two-center shell model for a fissioning system.

In the dynamical calculations, variation of the collective coordinates can be considered by the coupled Langevin equations,

$$\begin{aligned} q_i^{(n+1)} &= q_i^{(n)} + \frac{1}{2} \mu_{ij}^{(n)}(\mathbf{q})(p_j^{(n)} + p_j^{(n+1)})\tau \\ p_i^{(n+1)} &= p_i^{(n)} - \tau \left[ \frac{1}{2} p_j^{(n)} p_k^{(n)} \left( \frac{\partial \mu_{jk}(\mathbf{q})}{\partial q_i} \right)^{(n)} \right. \\ &\quad \left. - Q_i^{(n)}(\mathbf{q}) - \gamma_{ij}^{(n)}(\mathbf{q}) \mu_{ik}^{(n)}(\mathbf{q}) p_k^{(n)} \right] \\ &\quad + \theta_{ij}^{(n)} \xi_j^{(n)} \sqrt{\tau}, \end{aligned} \quad (1)$$

where  $m_{ij}$  ( $\|\mu_{ij}\| = \|m_{ij}\|^{-1}$ ) is the tensor of inertia,  $q_i$  and  $p_i$  are the collective coordinates and momenta conjugate to them,  $\theta_{ij}\xi_j$  is a random force,  $\theta_{ij}$  is its amplitude,  $\xi_j$  is a random variable, and  $\gamma_{ij}$  is the friction tensor. The superscript  $n$  in Eq. (1) shows that the corresponding quantity is calculated at the instant  $t_n = n\tau$ , where  $\tau$  is the time step of integration of the Langevin equations.  $Q_i$  is a conservative force and can be given by the Helmholtz free-energy  $Q_i(\mathbf{q}, I, K) = -(\partial F / \partial q_i)_T$ . The Helmholtz free energy can be determined in terms of the potential energy and the level-density parameter as follows:

$$F(\mathbf{q}, I, K) = V(\mathbf{q}, I, K) - a(\mathbf{q})T^2. \quad (2)$$

In the Fermi gas model the conservation force is given by [38]

$$Q_i(\mathbf{q}, I, K) = -\partial V(\mathbf{q}, I, K) / \partial q_i + T^2 \partial a(\mathbf{q}) / \partial q_i, \quad (3)$$

where the deformation dependence of the level-density parameter can be expressed by  $a(\mathbf{q}) = 0.073A + 0.095A^{2/3}B_s(\mathbf{q})$ . The inertia tensor is calculated in the Werner-Wheeler approximation for the incompressible and irrotational flow [39].

At low excitation energy the potential energy can be calculated on the basis of the liquid drop model with considering shell correction as follows [40,41]:

$$\begin{aligned} V(\mathbf{q}, I, K, T) &= V_{\text{SH}}(\mathbf{q}, T) + V_{\text{LDM}}(\mathbf{q}) + E_{\text{rot}} \\ &= V_{\text{SH}}(\mathbf{q}, T) + [B_s(\mathbf{q}) - 1]E_s^0(A, Z) \\ &\quad + [B_c(\mathbf{q}) - 1]E_c^0(A, Z) + \frac{\hbar^2 I(I+1)}{2J_{\perp}(\mathbf{q})} + \frac{\hbar^2 K^2}{2J_{\text{eff}}(\mathbf{q})}, \end{aligned} \quad (4)$$

where  $E_s^0$  and  $E_c^0$  are the surface and Coulomb energies of a spherical nucleus,  $B_s(\mathbf{q})$  and  $B_c(\mathbf{q})$  are surface and Coulomb energy terms [40].  $E_{\text{rot}}$  is the rotational energy,  $I$  is the spin of a compound nucleus, and  $K$  is the projection of  $I$  on the symmetry axis of the nucleus.  $J_{\parallel}$  and  $J_{\perp}$  are the rigid body moments of inertia about and perpendicular to the symmetry axis and  $J_{\text{eff}}$  is the effective moment of inertia  $J_{\text{eff}} = [J_{\parallel}^{-1} - J_{\perp}^{-1}]^{-1}$ .  $V_{\text{SH}}(\mathbf{q}, T)$  is the shell correction energy that can be evaluated by the Strutinski method from the single-particle levels of the two-center shell model [42,43]. The shell correction can be given as

$$V_{\text{SH}}(\mathbf{q}, T) = E_{\text{shell}}^o(\mathbf{q})\Phi(T). \quad (5)$$

The shell correction energy at the zero temperature  $T = 0$  reduces to  $E_{\text{shell}}^o$ . The shell correction energy at the zero temperature can be calculated with the shell effects in total single-particle energy and the pairing energy as follows:

$$E_{\text{shell}}^o(\mathbf{q}, T = 0) = \sum_{n,p} [E_{\text{shell}}^{(n,p)}(\mathbf{q}) + E_{\text{pair}}^{(n,p)}(\mathbf{q})], \quad (6)$$

where  $E_{\text{shell}}^{(n,p)}(\mathbf{q})$  and  $E_{\text{pair}}^{(n,p)}(\mathbf{q})$  can be calculated by the BCS approximation and Strutinsky prescription [42,44,45]. In Eq. (5) factor  $\Phi(T)$  is the temperature dependence of the shell correction. Factor  $\Phi(T)$  can be calculated by [46]

$$\Phi(T) = \exp\left(-\frac{aT^2}{E_d}\right), \quad (7)$$

here  $E_d$  is the shell damping energy and  $a$  is the level-density parameter. The magnitude of  $E_d = 20$  MeV was suggested by Ignatyuk and his co-authors in Ref. [38]. In the present calculations, dissipation is generated through the chaos-weighted wall and window friction formula, which is described in Ref. [47].

The evolution of the  $K$ -collective coordinate in the dynamical calculations can be determined by [36]

$$dK = -\frac{\gamma_K^2 T^2}{2} \frac{\partial V}{\partial K} dt + \gamma_K I \xi(t) \sqrt{T} dt, \quad (8)$$

where  $\xi(t)$  is a random number as Eq. (1).  $\gamma_K$  is dissipation coefficient of  $K$ .  $\gamma_K$  for a system consisting of two nuclei connected by a neck (a dinucleus) can be determined by [36,48]

$$\gamma_K = \frac{1}{rR_N \sqrt{2\pi^3 n_0}} \sqrt{\frac{J_R |J_{\text{eff}}| J_{\parallel}}{J_{\perp}^3}}, \quad (9)$$

where  $r$  is the distance between the centers of mass of the nascent fragments,  $R_N$  is the neck radius,  $J_R = M_0 R^2 / 4$  for a reflection symmetric shape, and  $n_0 = 0.0263$  MeV zs fm<sup>-4</sup> [49]. By assuming a constant  $\gamma_K$ , the average of  $K(t)$  can be expressed as

$$\langle K(t) \rangle_{K_0} = K_0 \exp\left[-\frac{\gamma_K^2 T^2 \hbar^2}{2J_{\text{eff}}} (t - t_0)\right]. \quad (10)$$

Figure 2 shows the dissipation coefficient as a function of coordinate  $r/R_0$  for the compound nucleus <sup>236</sup>Np.

It should be mentioned that the magnitude of  $\gamma_K$  can be determined for a dinucleus according to Eq. (9). On the

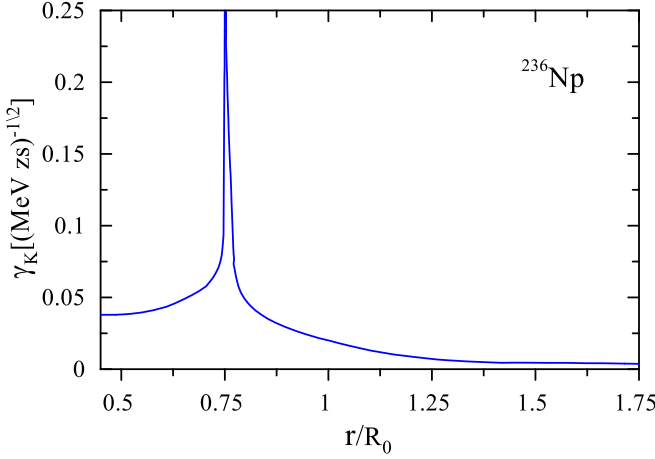


FIG. 2. The dissipation coefficient of  $K$  as a function of coordinate  $r/R_0$  for the compound nucleus  $^{236}\text{Np}$ .

other hand, in order to perform numerical integration of the Langevin equation for the  $K$  coordinate it is needed to determine the value of  $\gamma_K$  for all possible nuclear deformations. For mononuclear shapes the magnitude of  $\gamma_K$  can be determined by extrapolating Eq. (9).

In the calculations, the fission dynamics of a compound nucleus can be started from a spherical shape. The initial values of the collective coordinates  $\mathbf{q}_0$  and the momenta  $\mathbf{p}_0$  can be sampled by the Neumann method with the generating function,

$$\Phi(\mathbf{q}_0, \mathbf{p}_0, I_0, t = 0) \propto \exp\left[-\frac{V(\mathbf{q}_0) + E_{\text{coll}}(\mathbf{q}_0, \mathbf{p}_0)}{T}\right] \times \delta(\mathbf{q}_0 - \mathbf{q}_{\text{g.s.}}) \frac{d\sigma(I)}{dI}. \quad (11)$$

The spin distribution of compound nuclei produced in fission reactions  $d\sigma(I)/dI$  can be determined as [50]

$$\frac{d\sigma(I)}{dI} = \frac{2\pi}{k^2} \frac{2I + 1}{1 + \exp\left(\frac{I - I_c}{\delta I}\right)}, \quad (12)$$

here  $I_c$  is the critical spin and  $\delta I$  is the diffuseness parameter. The parameters  $I_c$  and  $\delta I$  can be obtained by the following relations [50]:

$$I_c = \sqrt{A_P A_T / A_{CN}} (A_P^{1/3} + A_T^{1/3}) (0.33 + 0.205 \sqrt{E_{\text{c.m.}} - V_c}), \quad (13)$$

and

$$\delta I = \begin{cases} (A_P A_T)^{3/2} \times 10^{-5} [1.5 + 0.02(E_{\text{c.m.}} - V_c - 10)] & \text{for } E_{\text{c.m.}} > V_c + 10, \\ (A_P A_T)^{3/2} \times 10^{-5} [1.5 - 0.04(E_{\text{c.m.}} - V_c - 10)] & \text{for } E_{\text{c.m.}} < V_c + 10, \end{cases} \quad (14)$$

when  $0 < E_{\text{c.m.}} - V_c < 120$  MeV; and when  $E_{\text{c.m.}} - V_c > 120$  MeV the term in the last brackets is put equal to 2.5.  $A_T$ ,  $A_P$  and  $A_{CN}$  represent the mass number of the target, projectile and the compound nucleus, respectively. Figure 3 shows the spin distribution for  $^{236}\text{Np}$  produced in the  $p + ^{235}\text{U}$

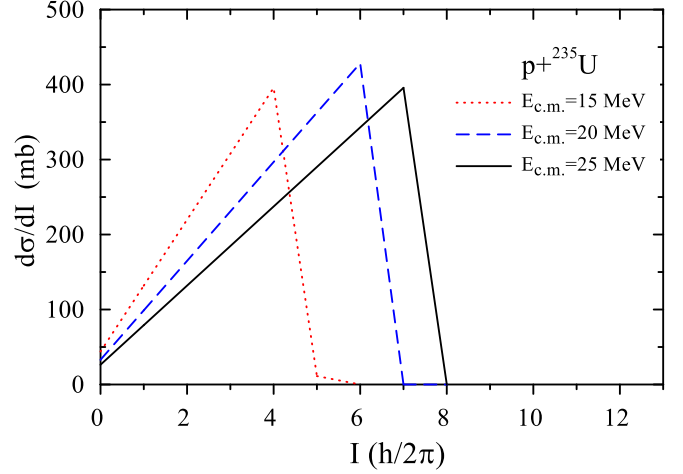


FIG. 3. The spin distribution of the compound nucleus  $^{236}\text{Np}$  produced in the  $p + ^{235}\text{U}$  reaction at  $E_{\text{c.m.}} = 15, 20,$  and  $25$  MeV.

reaction, for example, for projectile energy  $E_{\text{c.m.}} = 15, 20,$  and  $25$  MeV. It can be seen from Fig. 3 that at higher center-of-mass energy of the projectile the compound nucleus formed with a larger value of spin.

It should be mentioned that the initial spin  $I$  for each Langevin trajectory can be sampled from the spin distribution. Furthermore, in the present paper the initial projection of spin about the symmetry axis  $K$  is assumed to be equal to zero.

During evolution of a fissioning nucleus, the total excitation energy of nucleus can be determined by conservation of energy,

$$E^* = E_{\text{int}}(t) + E_{\text{coll}}(\mathbf{q}, \mathbf{p}) + V(\mathbf{q}, I, K) + E_{\text{evap}}(t), \quad (15)$$

here  $E_{\text{coll}} = 0.5\mu_{ij}(\mathbf{q})p_i p_j$  is the kinetic energy of the collective motion of the nucleus,  $E_{\text{int}}$  is the intrinsic excitation energy of the nucleus,  $E_{\text{evap}}(t)$  is the energy carried away by evaporated particles by time  $t$ , and  $V(\mathbf{q}, I, K)$  is the potential energy of the compound nucleus.

Evaporation of prescission particles and the  $\gamma$  particle from a compound nucleus are taken into account by using a Monte Carlo simulation technique. The decay widths for neutron, proton,  $\alpha$  particles, and  $\gamma$ -ray emission are calculated at each Langevin time-step  $\tau$  as in Refs. [51,52]. In the simulation of the evolution of a fissile nucleus a Langevin trajectory either reaches the scission point in which case it is counted as a fission event, or if the excitation energy reaches the value of  $E_{\text{int}} + E_{\text{coll}} < \min(B_n, B_f)$ , the event is counted as an evaporation residue ( $B_n$  is the binding energy of neutron and  $B_f$  is the fission barrier height). In the calculations, the scission point can be defined as the configuration in which the neck radius becomes zero.

In the present research, the deformation effects in determination of the binding energy of particles are considered as in Refs. [53–56]. Binding energies of the emitted particles can be obtained as

$$B_v(\mathbf{q}) = M_p(\mathbf{q}) - M_d(\mathbf{q}) - M_v, \quad (16)$$

here  $M_v$  is the mass of the emitted particle.  $M_p(\mathbf{q})$  is the mass of the mother, and  $M_d(\mathbf{q})$  is the mass of the daughter

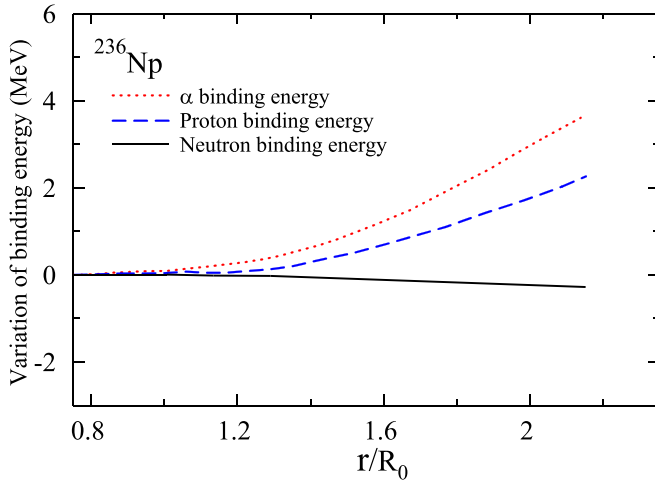


FIG. 4. Variation of the  $\alpha$ , proton, and neutron binding energies versus coordinate  $r/R_0$  relative to the spherical binding energies for  $^{236}\text{Np}$ .

nucleus. The results of calculations for change in  $\alpha$ , proton, and neutron binding energies as a function of  $r/R_0$  for  $^{236}\text{Np}$  are presented in Fig. 4. It is clear from Fig. 4 that the proton and  $\alpha$ -particle binding energies increase quickly with deformation whereas the neutron binding energy decreases slowly. It can be explained as follows; for a constant deformation the emission of a neutron causes a small decrease in the nuclear deformation energy, but the emission of charge particles causes a fast increase.

### III. RESULTS AND DISCUSSIONS

A stochastic approach based on 4D Langevin equations has been used to calculate the average number of neutrons

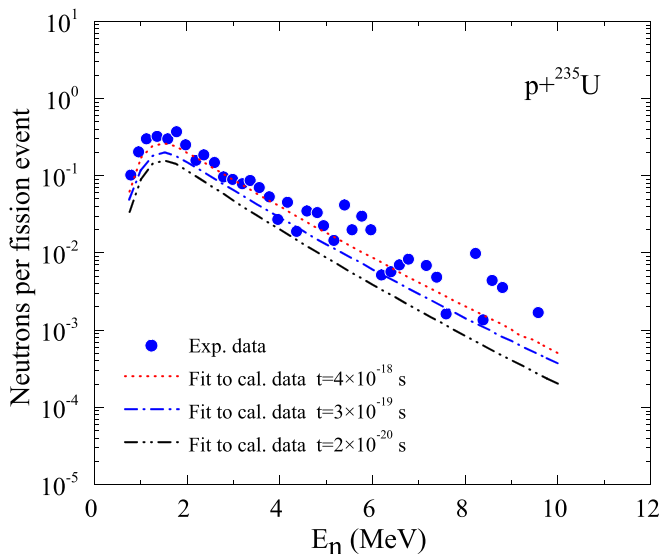


FIG. 5. The results of the average neutron per fission event as a function of neutrons emission energy for  $^{236}\text{Np}$  produced in the  $p + ^{235}\text{U}$  reaction with  $E_p = 12.7$  MeV. The solid circles are experimental data [57].

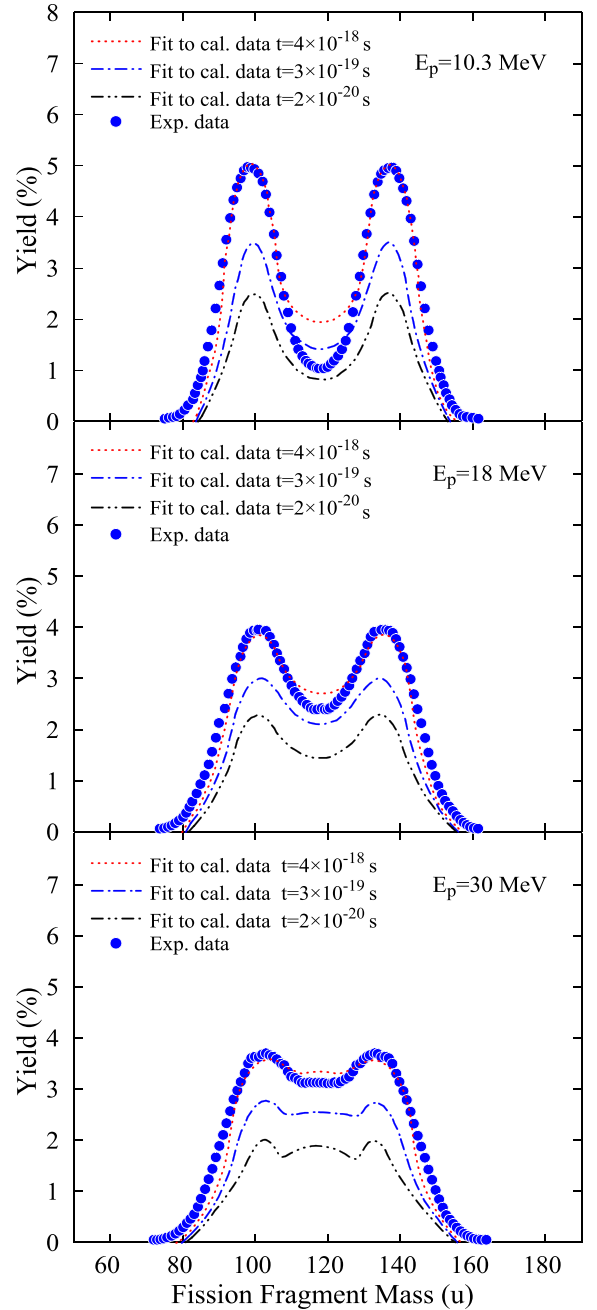


FIG. 6. The results of the time evolution of mass distribution of fission fragments of  $^{236}\text{Np}$  produced in the  $p + ^{235}\text{U}$  reaction with  $E_p = 10.3, 18,$  and  $30$  MeV. The solid circles are experimental data [58].

emitted per fission, the mass distributions of fission fragments, the average masses of heavy fragments, and the average total kinetic energies of fragments from fission  $^{236}\text{Np}$  produced in the  $p + ^{235}\text{U}$  reaction at  $10.3 \leq E_p \leq 30.0$  MeV. A benefit of the 4D dynamical model on the basis of Langevin equations is that one can investigate the timescale of the fission process. In simulation of the fission process of the excited nuclei the timescale is a very important parameter because the time-dependent decay rate is governed by the nuclear collective dynamics. The emission of precession

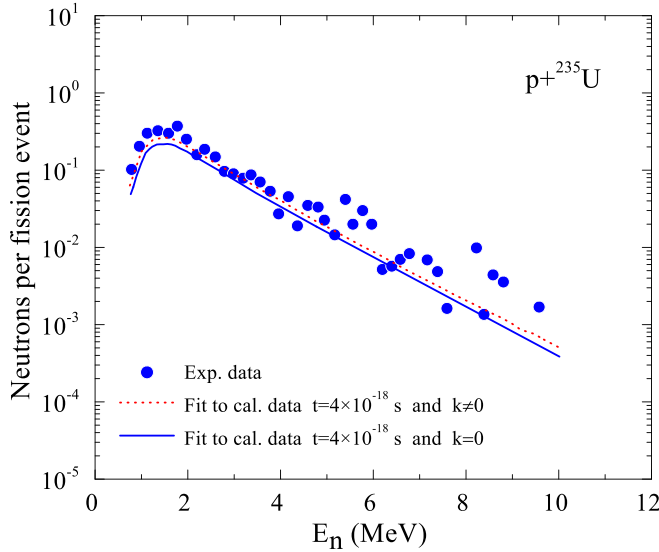


FIG. 7. The results of the average neutron per fission event as a function of neutrons emission energy for  $^{236}\text{Np}$  produced in the  $p + ^{235}\text{U}$  reaction calculated with and without considering the effect of projection of spin at  $E_p = 12.7$  MeV and  $t = 4 \times 10^{-18}$  s. The solid circles are experimental data [57].

particles as a process competing with fission changes the excitation energy of the fissioning system, and so it affects many characteristics of the fission process of the excited nuclei. Figure 5 shows the results of the average neutron per fission event as a function of neutron emission energy and with considering different timescales of the fission process for  $^{236}\text{Np}$  produced in the  $p + ^{235}\text{U}$  reaction with  $E_p = 10.3$ –30 MeV. Figure 6 also shows the results of the time evolution of the mass yields of fission fragments of  $^{236}\text{Np}$  produced with  $E_p = 10.3, 18,$  and 30 MeV. It should be mentioned that for each timescale of the fission process that used in the present calculations only the Langevin trajectories that reached the scission point have been considered as a fission event.

It is clear from Figs. 5 and 6 that the results of calculations quantitatively agree with the experimental data for  $t = 4 \times 10^{-18}$  s. It was also found that the number of fission events increases with time and almost all of the fission events occur dynamically until  $t = 4 \times 10^{-18}$  s and that the number of fission events becomes saturated. Furthermore, it can be seen from Fig. 6 that the positions and widths of the peaks are also reproduced with high accuracy.

It should be mentioned that in the simulation of the fission process of a compound nucleus, it is very important to consider the effect of projection of spin  $K$ . It can be investigated, for example, by estimation of the pre-scission neutron multiplicity. Figure 7 shows the results of the average neutron per fission event as a function of neutrons emission energy calculated for  $^{236}\text{Np}$  with and without considering the effect of projection of the spin. It is clear from Fig. 7 that with considering the effect of projection of spin the pre-scission neutron multiplicity increased for  $^{236}\text{Np}$ .

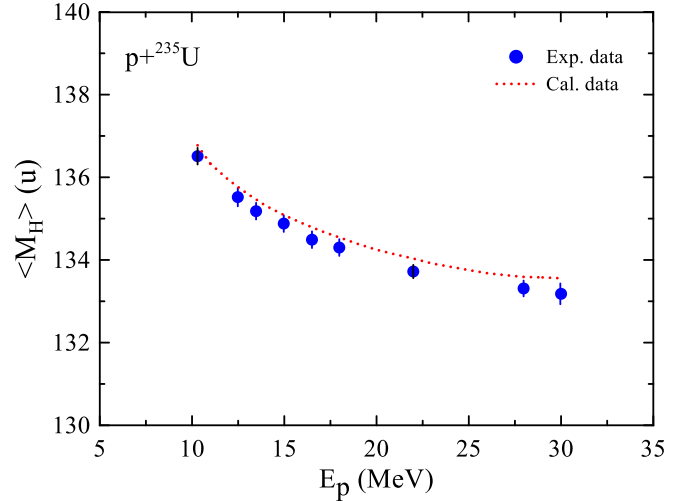


FIG. 8. The results of the average masses of heavy fragments of fission fragments of  $^{236}\text{Np}$  produced in the  $p + ^{235}\text{U}$  reaction with  $E_p = 10.3$ –30 MeV. The solid circles are experimental data [57].

In the present research, the average masses of heavy fragments ( $\langle M_H \rangle$ ) and the average total kinetic energies of fragments ( $\langle E_K \rangle$ ) have also been calculated for fission of  $^{236}\text{Np}$  with considering the time evolution of the compound nucleus equal to  $t = 4 \times 10^{-18}$  s. Figures 8 and 9 show the results of ( $\langle M_H \rangle$ ) and ( $\langle E_K \rangle$ ) from fission of  $^{236}\text{Np}$  produced in the  $p + ^{235}\text{U}$  reaction with  $E_p = 10.3$ –30 MeV. Figures 8 and 9 illustrate how proton energy influences the values of the average masses of heavy fragments and the average total kinetic energies of fission fragments of  $^{236}\text{Np}$  with  $E_p = 10.3$ –30 MeV. It can be seen from Figs. 8 and 9 that the average masses of heavy fragments and the average total kinetic energies of fission fragments of  $^{236}\text{Np}$  decrease with increasing projectile energy. In other words with increasing

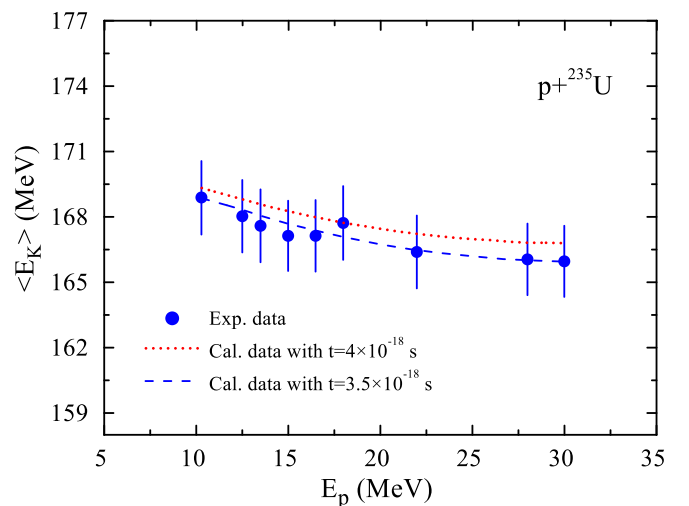


FIG. 9. The results of the average total kinetic energies of fission fragments from fission of  $^{236}\text{Np}$  produced in the  $p + ^{235}\text{U}$  reaction with  $E_p = 10.3$ –30 MeV. The solid circles are experimental data [57].



excitation energy of the compound system, the fragments approach symmetric fission. It can also be seen from Figs. 8 and 9 that the results of calculations for the average masses of heavy fragments quantitatively agree with the experimental data, although the results of calculations for the average total kinetic energies of fission fragments are slightly higher than the experimental data.

The average total kinetic energies of fission fragments of  $^{236}\text{Np}$  can be reproduced more conveniently by reducing the fission time. It can be seen from Fig. 9 that the experimental data for the average total kinetic energies of fission fragments of  $^{236}\text{Np}$  can be satisfactorily reproduced by using  $t = 3.5 \times 10^{-18}$  s. Actually, by reducing fission time decreases pre-scission particles multiplicity and, therefore, decreases average total kinetic energies of fission fragments.

#### IV. CONCLUSIONS

In the framework of the 4D Langevin equations have been calculated the average number of neutrons emitted per fission, the mass distributions of fission fragments, the average masses of heavy fragments, and the average total kinetic energies of fission fragments for the compound nucleus  $^{236}\text{Np}$  produced in the  $p + ^{235}\text{U}$  reaction at  $10.3 \leq E_p \leq 30.0$  MeV. In the dynamical calculations, dissipation was generated through the

chaos-weighted wall and window friction formula and dissipation coefficient of  $K$  was considered as a nonconstant parameter. Comparison of the calculated data for the above-mentioned quantities with the experimental data showed that the results of calculations are in good agreement with the experimental data, although the results of calculations for the average total kinetic energies of fission fragments are slightly higher than the experimental data. It was also shown that the number of fission events increases with time, and almost all of the fission events occur dynamically until  $t = 4 \times 10^{-18}$  s and that the number of fission events becomes saturated. It was also shown that the average total kinetic energies of fission fragments of  $^{236}\text{Np}$  can be reproduced more conveniently by using  $t = 3.5 \times 10^{-18}$  s. Furthermore, it was shown that the average masses of heavy fragments and the average total kinetic energies of fission fragments of  $^{236}\text{Np}$  decrease with increasing projectile energy. In other words with increasing excitation energy of the compound system, the fragments approach symmetric fission.

#### ACKNOWLEDGMENTS

I thank the anonymous referee for comments and suggestions, which led to a significantly improved version of this paper. Support for the Research Committee of the Persian Gulf University is greatly acknowledged.

- 
- [1] O. Hahn and F. Straßmann, *Naturwissenschaften* **27**, 11 (1939).
  - [2] L. Meitner and O. R. Frisch, *Nature (London)* **143**, 239 (1939).
  - [3] M. D. Usang, F. A. Ivanyuk, C. Ishizuka, and S. Chiba, *Sci. Rep.* **9**, 1525 (2019).
  - [4] M. D. Usang, F. A. Ivanyuk, C. Ishizuka, and S. Chiba, *Phys. Rev. C* **96**, 064617 (2017).
  - [5] H. Eslamizadeh and H. Razazzadeh, *Phys. Lett. B* **777**, 265 (2018).
  - [6] H. Eslamizadeh, *Phys. Rev. C* **94**, 044610 (2016).
  - [7] P. Jaffke, P. Möller, P. Talou, and A. J. Sierk, *Phys. Rev. C* **97**, 034608 (2018).
  - [8] J. Tian, N. Wang, and W. Ye, *Phys. Rev. C* **95**, 041601(R) (2017).
  - [9] N. Wang and W. Ye, *Phys. Rev. C* **97**, 014603 (2018).
  - [10] V. T. Maslyuk, O. O. Parlag, M. I. Romanyuk, O. I. Lendyel, and T. J. Marinetc, *EPL* **119**, 12001 (2017).
  - [11] H. Eslamizadeh, *Ann. Nucl. Energy* **38**, 2806 (2011).
  - [12] A. N. Andreyev, K. Nishio, and K.-H. Schmidt, *Rep. Prog. Phys.* **81**, 016301 (2018).
  - [13] H. Eslamizadeh and M. Soltani, *Ann. Nucl. Energy* **80**, 261 (2015).
  - [14] H. Eslamizadeh and N. Abdollahi, *Phys. Rev. C* **97**, 024614 (2018).
  - [15] W. Ye, *Phys. Rev. C* **81**, 011603(R) (2010).
  - [16] H. Eslamizadeh, *Pramana* **81**, 807 (2013).
  - [17] H. Eslamizadeh and E. Ahadi, *Phys. Rev. C* **96**, 034621 (2017).
  - [18] V. Y. Denisov, T. O. Margitych, and I. Y. Sedykh, *Nucl. Phys. A* **958**, 101 (2017).
  - [19] H. Eslamizadeh, *Pramana* **80**, 621 (2013).
  - [20] D. Naderi, S. A. Alavi, and V. Dehghani, *Int. J. Mod. Phys. E* **28**, 1950077 (2019).
  - [21] Yu. A. Lazarev, I. I. Gontchar, and N. D. Mavlitov, *Phys. Rev. Lett.* **70**, 1220 (1993).
  - [22] I. I. Gontchar, N. A. Ponomarenko, V. V. Turkin, and L. A. Litnevsky, *Phys. At. Nucl.* **67**, 2080 (2004).
  - [23] F. A. Ivanyuk, S. Chiba, and Y. Aritomo, *Phys. Rev. C* **90**, 054607 (2014).
  - [24] G. R. Tillack, R. Reif, A. Schülke, P. Fröbrich, H. J. Krappe, and H. G. Reusch, *Phys. Lett. B* **296**, 296 (1992).
  - [25] G. I. Kosenko, D. V. Vanin, and G. D. Adeev, *Yad. Fiz.* **61**, 2142 (1998).
  - [26] M. D. Usang, F. A. Ivanyuk, C. Ishizuka, and S. Chiba, *Phys. Rev. C* **94**, 044602 (2016).
  - [27] A. J. Sierk, *Phys. Rev. C* **96**, 034603 (2017).
  - [28] D. V. Vanin, P. N. Nadochdy, G. I. Kosenko, and G. D. Adeev, *Phys. At. Nucl.* **63**, 1865 (2000).
  - [29] G. I. Kosenko, I. I. Gonchar, O. I. Serdyuk, and N. I. Pischasov, *Yad. Fiz.* **55**, 920 (1992).
  - [30] I. I. Gontchar, A. E. Gettinger, L. V. Guryan, and W. Wagner, *Phys. At. Nucl.* **63**, 1688 (2000).
  - [31] P. N. Nadochdy, G. D. Adeev, and A. V. Karpov, *Phys. Rev. C* **65**, 064615 (2002).
  - [32] A. V. Karpov, P. N. Nadochdy, D. V. Vanin, and G. D. Adeev, *Phys. Rev. C* **63**, 054610 (2001).
  - [33] A. V. Karpov, R. M. Hiryanov, A. V. Sagdeev, and G. D. Adeev, *J. Phys. G: Nucl. Part. Phys.* **34**, 255 (2007).
  - [34] G. Chaudhuri and S. Pal, *Phys. Rev. C* **65**, 054612 (2002).
  - [35] J. P. Lestone, *Phys. Rev. C* **59**, 1540 (1999).
  - [36] J. P. Lestone and S. G. McCalla, *Phys. Rev. C* **79**, 044611 (2009).
  - [37] J. Maruhn and W. Greiner, *Z. Phys.* **251**, 431 (1972).
  - [38] A. V. Ignatyuk, G. N. Smirenkin, and A. S. Tishin, *Sov. J. Nucl. Phys.* **21**, 255 (1975).

- [39] K. T. R. Davies, A. J. Sierk, and J. R. Nix, *Phys. Rev. C* **13**, 2385 (1976).
- [40] H. J. Krappe, J. R. Nix, and A. J. Sierk, *Phys. Rev. C* **20**, 992 (1979).
- [41] A. J. Sierk, *Phys. Rev. C* **33**, 2039 (1986).
- [42] V. M. Strutinsky, *Nucl. Phys. A* **95**, 420 (1967).
- [43] S. G. Nilsson, C. F. Tsang, A. Sobiczewski, Z. Szymański, S. Wycech, C. Gustafson, I. L. Lamm, P. Möller, and B. Nilsson, *Nucl. Phys. A* **131**, 1 (1969).
- [44] V. M. Strutinsky, *Nucl. Phys. A* **122**, 1 (1968).
- [45] M. Brack, J. Damgaard, A. S. Jensen, H. C. Pauli, V. M. Strutinsky, and C. Y. Wong, *Rev. Mod. Phys.* **44**, 320 (1972).
- [46] T. Asano, T. Wada, M. Ohta, T. Ichikawa, S. Yamaji, and H. Nakahara, *J. Nucl. Radiochem. Sci.* **5**, 1 (2004).
- [47] H. Eslamizadeh, *J. Phys. G: Nucl. Part. Phys.* **39**, 085110 (2012).
- [48] S. G. McCalla and J. P. Lestone, *Phys. Rev. Lett.* **101**, 032702 (2008).
- [49] T. Døssing and J. Randrup, *Nucl. Phys. A* **433**, 215 (1985).
- [50] P. Fröbrich and I. I. Gontchar, *Phys. Rep.* **292**, 131 (1998).
- [51] M. Blann, *Phys. Rev. C* **21**, 1770 (1980).
- [52] J. E. Lynn, *The Theory of Neutron Resonance Reactions* (Clarendon, Oxford, 1968), p. 325.
- [53] P. Möller, J. R. Nix, W. D. Myers, and W. J. Swiatecki, *At. Data Nucl. Data Tables* **59**, 185 (1995).
- [54] N. Wang and W. Ye, *Phys. Rev. C* **87**, 051601(R) (2013).
- [55] P. Möller, W. D. Myers, W. J. Swiatecki, and J. Treiner, *Atomic Data and Nuclear Data Tables* **39**, 225 (1988).
- [56] K. Pomorski, J. Bartel, J. Richert, and K. Dietrich, *Nucl. Phys. A* **605**, 87 (1996).
- [57] M. Strecker, R. Wien, P. Plischke, and W. Scobel, *Phys. Rev. C* **41**, 2172 (1990).
- [58] S. I. Mulgin, S. V. Zhdanov, N. A. Kondratiev, K. V. Kovalchuk, and A. Ya. Rusanov, *Nucl. Phys. A* **824**, 1 (2009).